

# Characterization of PicoGreen Interaction with dsDNA and the Origin of Its Fluorescence Enhancement upon Binding

A. I. Dragan,<sup>†</sup> J. R. Casas-Finet,<sup>§</sup> E. S. Bishop,<sup>§</sup> R. J. Strouse,<sup>§</sup> M. A. Schenerman,<sup>§</sup> and C. D. Geddes<sup>†‡\*</sup>

<sup>†</sup>Institute of Fluorescence and <sup>‡</sup>Department of Chemistry, University of Maryland, Baltimore County, Maryland; and <sup>§</sup>MedImmune, Gaithersburg, Maryland

**ABSTRACT** PicoGreen is a fluorescent probe that binds dsDNA and forms a highly luminescent complex when compared to the free dye in solution. This unique probe is widely used in DNA quantitation assays but has limited application in biophysical analysis of DNA and DNA-protein systems due to limited knowledge pertaining to its physical properties and characteristics of DNA binding. Here we have investigated PicoGreen binding to DNA to reveal the origin and mode of PicoGreen/DNA interactions, in particular the role of electrostatic and nonelectrostatic interactions in formation of the complex, as well as demonstrating minor groove binding specificity. Analysis of the fluorescence properties of free PicoGreen, the diffusion properties of PG/DNA complexes, and the excited-state lifetime changes upon DNA binding and change in solvent polarity, as well as the viscosity, reveal that quenching of PicoGreen in the free state results from its intramolecular dynamic fluctuations. On binding to DNA, intercalation and electrostatic interactions immobilize the dye molecule, resulting in a >1000-fold enhancement in its fluorescence. Based on the results of this study, a model of PicoGreen/DNA complex formation is proposed.

## INTRODUCTION

Fluorescent probes that can interact with nucleic acids play an increasingly important role in biophysical studies of biological macromolecules and their complexes, in a variety of biomedical assays and in bioanalytical techniques. The most prominent fluorescent dyes introduced into biomedical research nearly a decade ago are PicoGreen (PG) and SYBR Green I (SG) (1–4). Even without a detailed knowledge of their spectral properties and mode of nucleic acid binding, they have been successfully applied to DNA quantitation in solution and gels, real-time PCR, cell chromosome staining and other techniques (1–10), due to the dramatic increase in their fluorescent emission upon interaction with double-stranded DNA (dsDNA).

Despite the many years of intensive use, the structures of PG and SG were only recently determined using a combination of mass spectroscopy and NMR (4). The chemical structure of PicoGreen is (2-(*n*-bis-(3-dimethylaminopropyl)-amino)-4-(2,3-dihydro-3-methyl-(benzo-1,3-thiazol-2-yl)-methylidene)-1-phenyl-quinolinium). Knowledge of the PG and SG structures has given the opportunity for quantitative studies of their binding to DNA. On binding DNA, PG fluorescence increases >1000-fold (3,7) and this is proportional to the quantity of DNA present, up to concentrations of several picograms/mL, which serves as the basis for nucleic acid quantitation assays. An interesting feature of PG is its ability to strongly bind not only to highly polymeric DNA but also to short duplexes <20 bp, likewise exhibiting a sensitivity in the picogram range (7,11). This ultimately explains its high effectiveness as a DNA-quantifier in real-time PCR, in following DNA digestion kinetics

(6), in host cell DNA assays (11), and even when small fragments of DNA duplex need to be detected.

In the presence of silver nanoparticles, the fluorescence of PG in complex with DNA is enhanced ~38,000-fold, as compared to free PG, due to the metal-enhanced fluorescence effect (12). This remarkable metal-enhanced fluorescence effect was first observed in our laboratory and significantly expands the fluorescence applications of PG to a broad area of biomedical assays that use DNA quantitation (7).

Despite the fact that the unique fluorescence properties of PG are now extensively exploited in analytical applications, no detailed physical characterization of PG binding to DNA has been carried out to determine the origin of its drastic fluorescence enhancement upon association. In particular, no structure has been published, by crystallography or NMR, of PG or of SG, nor of ethidium bound to a DNA duplex (for ethidium there is only general concept of the dye/DNA complex, which was formulated on the basis of x-ray crystallographic studies of ethidium-dinucleoside monophosphate crystalline complexes (13)). The lack of sequence specificity in the DNA binding of these dyes represents a major impediment to determination of a bound structure at atomic resolution.

To use PG as a research tool for DNA quantitation in solution and also for precise biophysical studies of complex biomacromolecular structures, it is important to obtain biophysical data that could lead to further understanding of how these dyes bind to DNA and why such a large increase in fluorescence results from binding. To do this requires determination of binding constants, i.e., the Gibbs energy of interaction, the size of the binding site, the relative involvement of electrostatic and nonelectrostatic forces in

Submitted March 3, 2010, and accepted for publication September 3, 2010.

\*Correspondence: geddes@umbc.edu

Editor: David P. Millar.

© 2010 by the Biophysical Society  
0006-3495/10/11/3010/10 \$2.00

doi: 10.1016/j.bpj.2010.09.012

PG/DNA complex stabilization, and the mode of binding (intercalation versus surface binding).

In analytical assays, competition with PG from various DNA-binders (drugs, proteins, etc.) can interfere with quantitative assays, so it is particularly important to understand where and how PG binds to DNA: in the minor or major groove, with or without intercalation? Answers to these questions are particularly important for enhancing the utility of PG in research.

In this study, we have explored these questions and have been able to propose an outline model for the PG/DNA complex.

## MATERIALS AND METHODS

The *Escherichia coli* DNA and Hoechst 33258 were purchased from Sigma-Aldrich (St. Louis, MO), ethidium bromide (EB), PicoGreen (PG), and SYBR Green I (SG) dyes were purchased from Invitrogen. The concentration of EB, Hoechst, PG, and SG were determined by measuring the optical density of the solutions using extinction coefficients of  $E_{480} = 5600 \text{ M}^{-1} \text{ cm}^{-1}$ ,  $E_{245} = 46,000 \text{ M}^{-1} \text{ cm}^{-1}$ ,  $E_{500} = 70,000 \text{ M}^{-1} \text{ cm}^{-1}$  and  $75,000 \text{ M}^{-1} \text{ cm}^{-1}$ , respectively (3). (Note that the structure of PicoGreen having been determined (4), the IUPAC (*International Union of Pure and Applied Chemistry*) name is (2-(*n*-bis-(3-dimethylaminopropyl)-amino)-4-(2,3-dihydro-3-methyl-(benzo-1,3-thiazol-2-yl)-methylidene)-1-phenyl-quinolinium) and the molecular mass = 552.5 Da.)

The 50-bp DNA sequence used in this study is a fragment of an Alu sequence taken from Chinese hamster ovary cells:

5' – <sup>1</sup>GAG ATA TGA GCA AAA GAA ACT TGG AAA  
GGA GGC TGG AGA GAT GGC TCG AG<sup>50</sup> – 3'.

Complementary 50 base oligonucleotides were purchased from Integrated DNA Technologies (Coralville, IA) and additionally purified by anion-exchange *fast protein liquid chromatography* on a Mono-Q column (Amersham Pharmacia Biotech, Piscataway, NJ), using a linear 0.1–1.0 M NaCl gradient in 10 mM Tris-HCl buffer (pH 7.0), 1 mM EDTA, 20% acetonitrile. The DNA was precipitated with ethanol, then pelleted and air-dried. Concentrations of single strands and the duplex were determined from the  $A_{260}$  of the nucleotides after complete digestion by phosphodiesterase I (Sigma-Aldrich) in 100 mM Tris-HCl (pH 8.0) (15). The DNA duplex was prepared by mixing the complementary oligonucleotides in equimolar amounts, heating to 70°C, and then cooling slowly to room temperature. The molecular mass of the 16-bp dsDNA was 9825.4 Da. Solutions of duplex DNA for the experiments were prepared by extensive dialysis against the required buffer.

Fluorescence and excitation spectra of free PG and PG in complex with the DNA were measured on a Cary Eclipse (Varian, Cary, NC) spectrofluorimeter at room temperature. PG was excited at 485 nm and the fluorescence monitored over the wavelength range 490–800 nm. A 0.2-cm path-length Suprasil quartz cell (Hellma, Plainview, NY) was used.

The fluorescence excited state lifetimes of PG and SG in both the free state (in TE buffer, pH 7.6 and in TE/glycerol mixtures) and in complex with DNA was measured using a TemPro Fluorescence Lifetime System (Horiba Jobin Yvon, Edison, NJ). The reference cell contained colloidal silica and a Ludox SM-30 (Sigma-Aldrich) solution was used as a control (zero lifetime). Measurements were performed at room temperature.

Diffusion of the 50 bp DNA at different PG/DNA ratios was studied by measuring autocorrelation  $G(t)$ -functions using an Alba Fluorescence Correlation Spectrometer (ISS, Champaign, IL). Excitation of fluorescence used a 473-nm laser line. Measurements were performed in plastic 200  $\mu\text{L}$  wells (Nalge Nunc International, Rochester, NY).

Calculation of the Forster distance ( $R_o$ ) for fluorescence resonance energy transfer from the Hoechst 33258 to the PicoGreen dye was undertaken using the following well-known equations (16),

$$R_o = 9.79 \times 10^3 (k^2 n^{-4} \phi_D J)^{1/6}, \text{ \AA}, \quad (1)$$

$$J = \int_0^{\infty} F_D(\lambda) \times \epsilon_A(\lambda) \times \lambda^4 d\lambda, \quad (2)$$

where the factor  $k = 2/3$  assumes free rotation between the transition vectors of the donor and acceptor dyes;  $n = 1.333$  is the refractive index of the media (water);  $\phi_D = 0.42$  is the quantum yield of Hoechst in the complex with DNA (17); and  $J$  is the spectral overlap integral expressing the extent of overlap between the fluorescence spectra of a donor ( $F_D$ ) and the absorption spectra of an acceptor ( $\epsilon_A$ ). Absorption spectra of PicoGreen (PG) were recorded using a Varian spectrophotometer. In calculations the molar extinction coefficient of PG was taken as  $\epsilon_{495} = 75,000 \text{ M}^{-1} \text{ cm}^{-1}$  (4,17). The corrected fluorescence spectrum of Hoechst in complex with calf thymus DNA (Hoechst/DNA ratio 0.05 dyes/DNA bp) was determined using a Varian spectrofluorometer.

## RESULTS AND DISCUSSION

### Analysis of PG binding to free dsDNA

The fluorescence intensity of PG upon binding to DNA increases significantly (7), which makes it possible to study dye/DNA interactions. Assuming that the fluorescence intensity is a linear function of bound PG, the change in intensity as a function of the PG dye in solution can be employed to calculate the fraction of bound PG during DNA titration with the dye. The fraction of bound PG ( $\theta$ ) can be expressed as

$$\theta = (F - F_f) / (F_b - F_f), \quad (3)$$

where  $F$  is an observed fluorescence intensity of PG, and  $F_b$  and  $F_f$  are the fluorescence intensities of 100% bound and free PG in solution, respectively. Considering that  $F_b \gg F_f$  (the fluorescence in the bound state is >1000-fold greater than in the free state,  $F_b/F_f = 1100$  (7)), the contribution of free dye to the total observed signal is negligible, <0.1%, so Eq. 3 can be simplified to

$$\theta = F/F_b. \quad (4)$$

The concentration of free PG in solution at equilibrium can be written as

$$L = (1 - \theta)C_{PG}, \quad (5)$$

whereas the PG binding density, i.e., the number of bound PGs per DNA bp, is

$$\nu = \theta C_{PG} / C_{DNA}, \quad (6)$$

where  $C_{PG}$  and  $C_{DNA}$  are the total concentrations of PG and DNA in solution, respectively.

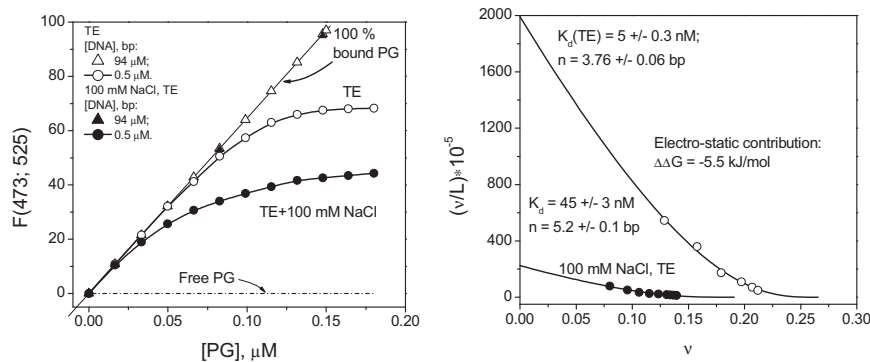


FIGURE 1 (Left) Isotherms of binding of PG to DNA in TE buffer and in 100 mM NaCl, TE, pH 7.6. (Right) PG binding to DNA plotted in Scatchard coordinates and fitted using Eq. 7.

The results of PG binding to 50 bp DNA (0.5  $\mu\text{M}$  (bp)) in TE buffer, pH 7.6 and in 100 mM NaCl, TE buffer are shown in Fig. 1 (left). The fluorescence intensity functions for the two ionic strengths employed are proportional to the change in the fraction of bound PG, according to Eq. 3. To calculate the fraction of the bound state ( $\theta$ ), the fluorescence of 100% bound PG was measured using a high concentration of DNA (94  $\mu\text{M}$  DNA (bp)). In this case, the fluorescence is a linear function of the PG concentration in solution.

Fig. 1 (right) presents binding isotherms of PG to DNA at two salt conditions plotted in Scatchard coordinates. Analysis of the experimental data was performed using the conditional probability model for noncooperative excluded site binding derived by McGhee and von Hippel (18). The analytical expression for PG binding to DNA is

$$v/L = K_a(1 - nv)^n / (1 - nv + v)^{(n-1)}, \quad (7)$$

where  $K_a$  is the intrinsic (observed) association constant and  $n$  is the size of the binding site in bp, i.e., the number of DNA basepairs excluded to another dye by each bound dye molecule. The data were fitted using a nonlinear least-squares fitting procedure where  $K_a$  and  $n$  were the fitted parameters. The binding parameters of PG thereby obtained are presented in Table 1.

The data in Table 1 demonstrate that association of PG with DNA is salt-dependent: the dissociation constant in TE is 5 nM but in TE plus 100 mM NaCl, it is  $\sim 10$ -fold greater,  $K_d = 45$  nM. The change in binding parameters with salt concentration is a manifestation of the electrostatic contribution to the Gibbs energy of PG/DNA interaction. Under the conditions used, the difference in the Gibbs

binding energy between low and high salt is  $\Delta\Delta G = 5.5$  kJ/mol and is in good agreement with the Gibbs energy estimated for one electrostatic contact, i.e.,  $\sim 5$  kJ/mol (19). Therefore, we propose that the positively charged group of PG forms an electrostatic contact with a DNA phosphate group. A more thorough analysis of electrostatic PG/DNA interactions is provided below.

The size of the PG binding site on DNA is  $n \approx 4$  bp and increases slightly at high salt concentration. Interestingly, the size of the PG binding site is larger than that for the classical intercalator, EB, which is  $\sim 2$  bp (Table 1). Assuming that PG and EB both intercalate into DNA in a similar manner, the observed size of the PG binding site is surprisingly large. On the other hand, the observed difference between the PG and EB site size could be explained by contacts of the additional molecular groups in PG to the DNA. This assumption is in agreement with a significantly stronger affinity of PG to DNA than that of EB (Table 1).

### Analysis of the electrostatic interactions in the PG/DNA complex

The observed dependence of the association constant upon the ionic strength of the solution is of great interest because it is indicative of the electrostatic forces that play a significant role in the association and stability of the PG/DNA complex, as expected for a positively charged ligand and macromolecular polyanion. The electrostatic interaction of a ligand with DNA, in fact, represents an entropic effect of the mixing of counterions released from DNA with ions in bulk solution (20–22), and the entropy of their mixing therefore depends on the concentration of the ions in solution. We studied the dependence of the PG/DNA association constant on salt concentration to reveal the contribution of electrostatic and nonelectrostatic components to the energy of the PG/DNA interaction (Fig. 2). If  $Z$  is the number of DNA phosphate groups that interact with the dye and  $\psi = 0.88$  is the number of cations ( $\text{Na}^+$ ) per phosphate group that are released upon ligand binding (21,22), their product,  $Z\psi$ , is the total number of tightly bound cations released

TABLE 1 DNA binding parameters for PicoGreen (PG) and ethidium bromide (EB)

Dye	TE buffer, pH 7.6		100 mM NaCl, TE buffer, pH 7.6		$\Delta\Delta G$ , kJ/mol
	$K_d$ , nM	$n$ , bp	$K_d$ , nM	$n$ , bp	
PG	$5.0 \pm 0.3$	$3.76 \pm 0.06$	$45.0 \pm 3.0$	$5.2 \pm 0.1$	5.5
EB	$870 \pm 25$	$2.80 \pm 0.02$	$5556 \pm 60$	$2.5 \pm 0.02$	4.6

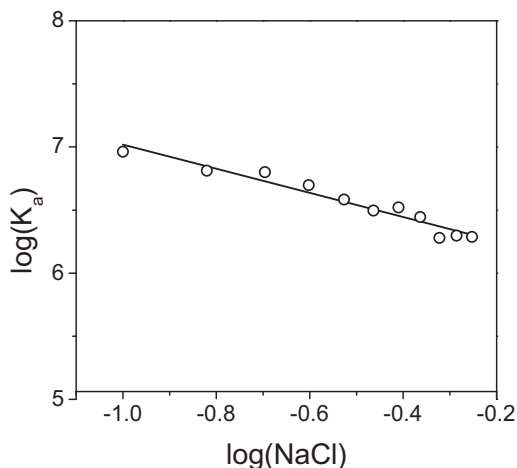


FIGURE 2 Dependence of the PG/DNA association constant ( $K_a$ ) upon NaCl concentration in solution. The slope of the dependence  $\log(K_a)$  versus  $\log(\text{NaCl})$  is  $Z\Psi = 0.95 \pm 0.07$ . The number of electrostatic contacts of PG with DNA is then  $Z = 1.1 \pm 0.1$ , taking  $\Psi = 0.88$ .

and the logarithm of the association constant can be presented as

$$\log(K) = \log(K_{\text{nel}}) - Z\Psi \times \log[\text{NaCl}], \quad (8)$$

or in terms of the Gibbs energy as

$$\Delta G = \Delta G_{\text{nel}} - Z\Psi \times RT \times \ln[\text{NaCl}], \quad (9)$$

assuming that the first term in Eq. 9,  $\Delta G_{\text{nel}}$ , results from nonelectrostatic interactions between PG and DNA and does not depend on the salt concentration; and the second term,  $\Delta G_{\text{el}} = -Z\Psi \times RT \times \ln[\text{NaCl}]$ , reflects the electrostatic component of the Gibbs energy, which originates from the release of counterions (19,23–25). The second term, i.e., the electrostatic component of the Gibbs energy, depends on the salt concentration and vanishes at the standard salt concentration (1 M NaCl) where association of the dye with DNA is stabilized entirely by van der Waals contacts, hydrogen-bonding, and dehydration effects—together comprising the nonelectrostatic component of the binding energy.

Fitting the data shown in Fig. 2 to Eq. 8 results in a slope of

$$\delta \log(K) / \delta [\text{NaCl}] = Z\Psi = 0.95 \pm 0.07$$

and the intercept with the Y axis at

$$\log[\text{NaCl}] = 0, \text{ i.e., } \log(K_{\text{nel}}) = 6.2 \pm 0.1.$$

From the slope, one can estimate the number of electrostatic contacts of PG with DNA phosphates as  $Z = 1.1 \pm 0.1$ , i.e., one electrostatic contact. The Gibbs energy of PG/DNA association at 100 mM NaCl can be written in terms of its nonelectrostatic and electrostatic components,

$$\Delta G = \Delta G_{\text{nel}} + \Delta G_{\text{el}} = -42 \text{ kJ/mol},$$

where  $\Delta G_{\text{nel}} = -37 \text{ kJ/mol}$  and  $\Delta G_{\text{el}} = -5 \text{ kJ/mol}$ . This suggests that most of the PG/DNA affinity originates from nonelectrostatic interactions, with the electrostatic component playing a minor role, perhaps important for maintaining conformational stabilization of the PG structural components on the DNA. Interestingly, the Gibbs energy of PG/DNA interaction is significantly larger than for EB binding to DNA ( $\Delta G = -30 \text{ kJ/mol}$ ; see Table 1). Because both dyes have a single electrostatic contact with DNA and consequently the same value of the electrostatic Gibbs energy, the difference is

$$\begin{aligned} \Delta \Delta G_{\text{nel}}^{(\text{PG/EB/DNA})} &= \Delta G_{\text{nel}}^{(\text{PG/DNA})} - \Delta G_{\text{nel}}^{(\text{EB/DNA})} \\ &\approx -12 \text{ kJ/mol}. \end{aligned}$$

A larger binding site size and nonelectrostatic Gibbs energy for PG correlate with each other, assuming that in addition to intercalation, the PG/DNA complex is further stabilized by multiple interactions between PG groups and DNA. Probable candidates for such additional contacts with DNA are the two armlike dimethyl-aminopropyl groups, the summed length of which approximates well to the increase in binding site noted for PG. It is worth noting that these elongated arms have similar structures to the well-known DNA-binding peptides that bind DNA in the minor groove termed “AT-hooks” (19). Moreover, the nonelectrostatic Gibbs energy of AT-hook binding to DNA is  $\sim -(12\text{--}14) \text{ kJ/mol}$  (19), which correlates well with our value of  $\Delta \Delta G_{\text{nel}}^{(\text{PG/EB/DNA})}$ .

### Fluorescence correlation spectroscopy study of DNA diffusion in the presence of PG

There is published data, obtained in hydrodynamic studies of SYBR Green (SG)/DNA complexes, that indicate an intercalation mode of SG binding to DNA (4). PG and SG have considerable structural similarity, which strongly suggests that PG intercalates into DNA upon association, but to date there are no direct experimental data. Consequently, we have used fluorescence correlation spectroscopy (FCS) to compare the diffusion of 50 bp DNA in the presence of PG and SG. FCS is a powerful technique for studying the mobility of macromolecules in solution based on the change in a molecule’s hydrodynamic radius and shape. In FCS experiments, one can observe the fluctuation in fluorescence intensity in a small focused confocal laser volume by comparing  $F(t)$  with  $F(t+\tau)$ , where  $\tau$  is a delay (lag) time, thereby calculating the correlation between them for a range of  $\tau$ -values. This results in an autocorrelation function,  $G(t)$ , of the fluorescence fluctuations which contains valuable information on the diffusion coefficient and fluorophore concentration,

$$G(t) = \langle F(t)F(t + \tau) \rangle / \langle F \rangle^2, \quad (10)$$

where  $\langle F \rangle$  is the mean intensity value. Additionally, the average number of molecules ( $N$ ) in the effective volume,  $V_{\text{eff}}$ , can be calculated from the  $G$ -function at  $\tau = 0$ :  $G(0) = 1/N$ , where  $N = [C] V_{\text{eff}}$ .

Unlike many hydrodynamic techniques, FCS needs fluorescence labeling of the studied macromolecules and is therefore incapable of measuring an autocorrelation function for naked DNA. We have measured autocorrelation  $G(\tau)$ -functions for 50-bp DNA/dye complexes at different PG/DNA ratios and the results are shown in Fig. 3. Progressive increase of the PG/DNA ratio shifts the  $G(\tau)$ -function to relatively longer diffusion times (Fig. 3 a), which consequently decreases the amplitude of the autocorrelation function,  $G(0)$  (Fig. 3 b). The observed change in  $G(0)$  is

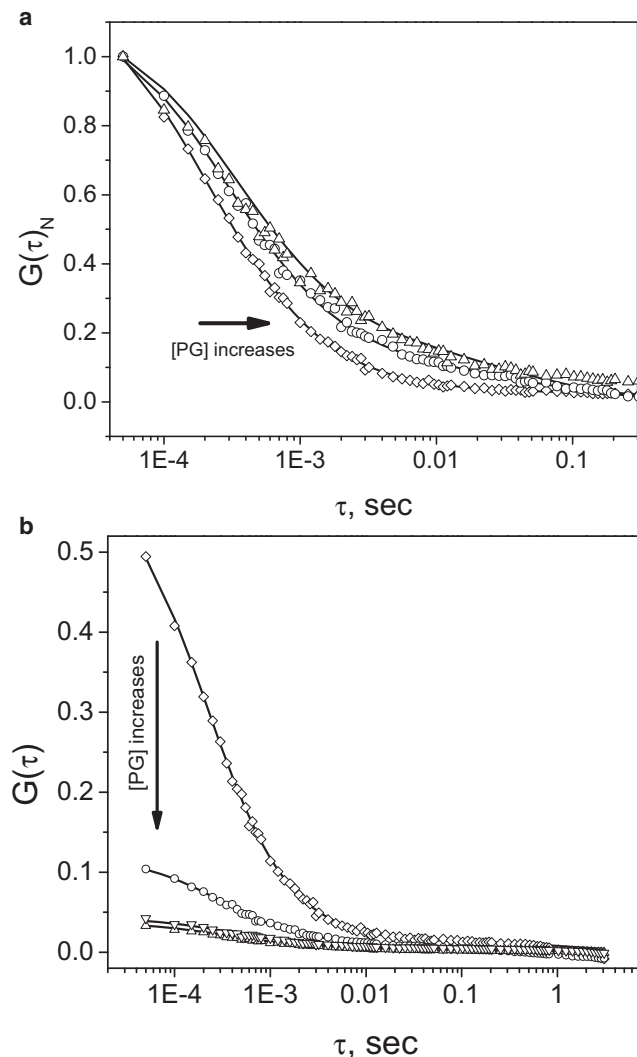


FIGURE 3 (a) Normalized autocorrelation functions for DNA in complex with PG at different PG/(DNA, bp) ratios, from 0.1 to 0.3. (b) Autocorrelation functions for the same samples as in panel a.

a direct reflection of PG binding to DNA; it is inversely proportional to the density of PG on DNA (the concentration of DNA in the experiment was held constant), and demonstrates saturation at high PG/DNA ratios  $>0.2$ . It should be noted that the  $G(\tau)$ -function shifts upon increased PG concentration and the change is nonlinear, resulting in saturation at high ( $>0.2$ ) PG/DNA ratios. The observed shift can be explained by an increase of the characteristic diffusion time of the complex,  $\tau_D$ . It has been shown that intercalation of a dye into a DNA duplex substantially increases the DNA interbase pair distance, and as a result, the total DNA length (4,26). This ultimately results in a decrease in the DNA diffusion coefficient ( $D$ ), which, for FCS experiments, is related to the characteristic diffusion time as

$$\tau_D = r_0^2 / (4D),$$

where  $r_0$  is the radius of the focal volume. For small DNA duplexes ( $L < 200$  bp), the diffusion time is approximately proportional to the length of the duplex (27). Autocorrelation functions for PG/DNA and SG/DNA complexes are compared in Fig. S1 and Fig. S2 in the Supporting Material: their profiles are very similar indeed, strongly suggesting the same mode of binding, i.e., intercalation.

#### Does PG bind to the DNA minor groove?

From the analysis of PG binding to DNA it is apparent that in addition to intercalation and electrostatic interaction with DNA phosphate groups, PG can also form extensive contacts within the DNA groove(s). These contacts contribute to the nonelectrostatic component of the Gibbs energy and significantly increase its affinity for the DNA. Despite certain differences in shape/size, both the major and minor grooves of the DNA can participate in ligand-DNA complex formation. To elucidate where PG enters DNA and to what DNA groove PG binds, we have studied the competition between PG and the DNA minor groove binder, Hoechst 33258. Hoechst 33258 is a well-known DNA binding agent that interacts preferentially with the minor groove of AT-rich sequences of a DNA duplex (28,29).

Fig. 4 (left) and Fig. 5 show the result of titrating DNA with Hoechst. Binding to DNA increases the intensity of Hoechst emission, which approaches saturation at a Hoechst/DNA ratio of  $\sim 0.05$ , i.e., implying an apparent binding site size of  $\sim 20$  bp. Using a preformed Hoechst/DNA complex with dye/DNA = 0.1, PG was titrated in, simultaneously monitoring the fluorescence of both Hoechst and PG using excitation at 350 nm, i.e., at a wavelength where both dyes absorb (Fig. 4 (center)). The fluorescence spectra of Hoechst and PG are well separated, which makes it possible to observe their separate changes during the experiment. It can be seen that, on adding PG to the Hoechst/DNA complex, the fluorescence of Hoechst

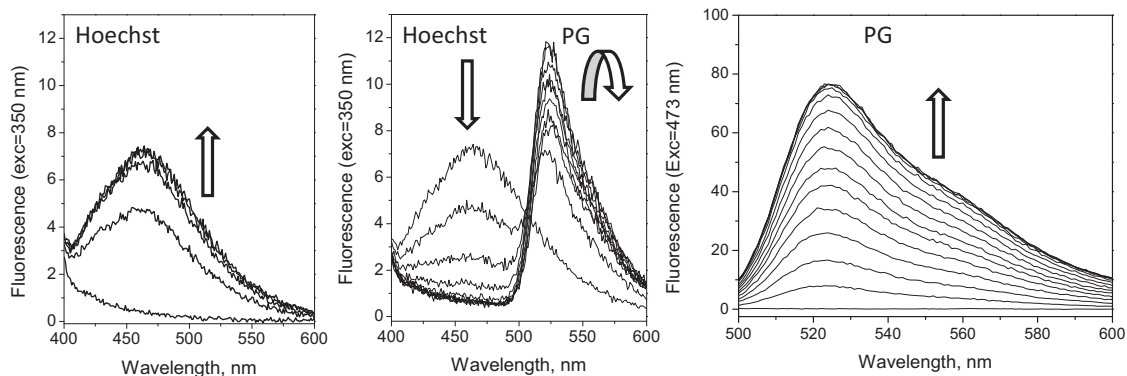


FIGURE 4 (Left) Change in fluorescence spectra of Hoechst 33258 upon binding to DNA. The ratio of Hoechst/DNA(bp) increases in equal steps from 0 to 0.13. Excitation of fluorescence was at 350 nm. (Center and right) Titration of DNA/Hoechst complex (Hoechst/DNA = 0.1) with PicoGreen. The PG/DNA (bp) ratio increases in equal steps from 0 to 0.3 (center) and from 0 to 0.47 (Right). Fluorescence spectra of Hoechst 33258 and PG were excited at 350 nm (center) and at 473 nm (right). (Arrows) Change in fluorescence intensity upon increase in concentration of the fluorophore.

decreases sharply and at PG/DNA > 0.15, asymptotically reaches a constant value (Fig. 6 (left)). Interestingly, a very different behavior is observed for PG: the intensity of the PG emission sharply increases to a maximum at ~0.1 PG/bp, then drops more gradually to a constant level (Fig. 6, right). We also monitored the fluorescence of PG during the titration using excitation at 472 nm, where only PG absorbs (Fig. 6 (left, red curve)). The observed changes in emission of Hoechst and PG suggest quite complex processes occur upon progressive increase of PG titrated into the solution of Hoechst/DNA complex. At first it would seem that competition between the dyes for DNA binding should result in similar profiles of fluorescence change for Hoechst and PG, but this is not what is observed. To understand this discrepancy, consider the PG fluorescence obtained using excitation at 350 nm, i.e., when both dyes are excited, Fig. 6 (right). The initial PG emission enhancement function follows the decrease of Hoechst fluorescence intensity such that the fluorescence of PG reaches a maximum value at the same PG/DNA ratio as Hoechst

emission at a minimum. This suggests two underlying processes. Further, an increase of the PG/DNA ratio results in a reduction of the PG fluorescence.

The difference in PG intensity change for the two excitation wavelengths could be explained if we assume that fluorescence resonance energy transfer (FRET) occurs between Hoechst and PG. In fact, the fluorescence emission spectrum of Hoechst considerably overlaps the absorption spectrum of PG (Fig. S3), making them a suitable donor-acceptor pair. Calculation of the Förster radius for the Hoechst-PG donor-acceptor (see Materials and Methods) gave  $R_0 = 42 \text{ \AA}$ . Due to preferential binding of Hoechst to AT-rich DNA sequences, the apparent size of the Hoechst binding site on DNA (~20 bp) is significantly larger than its real physical size of 4–5 bp (30), leaving a significant amount of uncomplexed free space on the DNA duplex. At the beginning of the titration, PG readily binds free DNA in between bound Hoechst sites of the Hoechst/DNA complex, because PG does not show preference for any DNA sequence. An average distance between Hoechst sites is ~20 bp, i.e., ~60 Å, which is comparable to the calculated Förster distance for resonance energy transfer from Hoechst to PG. Therefore, PG binding to free DNA at the beginning of the titration causes intensive FRET from the bound Hoechst (donor) to the PG (acceptor), resulting in a decrease of Hoechst emission accompanied by the enhancement of PG fluorescence. At this stage there is no effective competition between the dyes for binding to DNA. However, after saturation of free DNA space, PG starts to compete for DNA sites that have been preoccupied by Hoechst. Displacing the Hoechst dye from the DNA into bulk solution as a result of competition with PG dramatically increases the distance between donors and acceptors, and the FRET becomes negligible, ultimately leading to a reduction in PG fluorescence intensity observed when excited at 350 nm. When the PG fluorescence is excited at 472 nm and monitored at 525 nm, i.e., when there is no FRET from Hoechst to PG, a straightforward PG binding curve

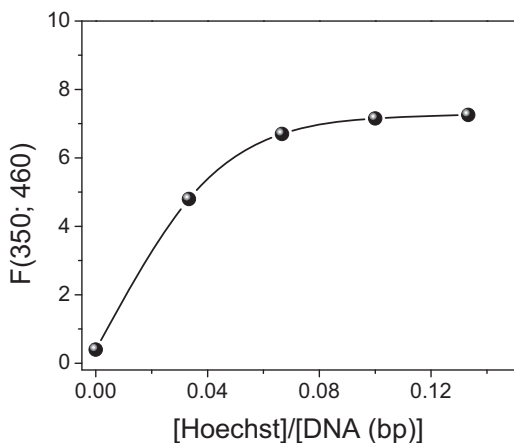


FIGURE 5 Isotherm of binding Hoechst 33258 to 50 bp DNA. The concentration of the dye was 0.5  $\mu\text{M}$  in TE buffer, pH 7.6.

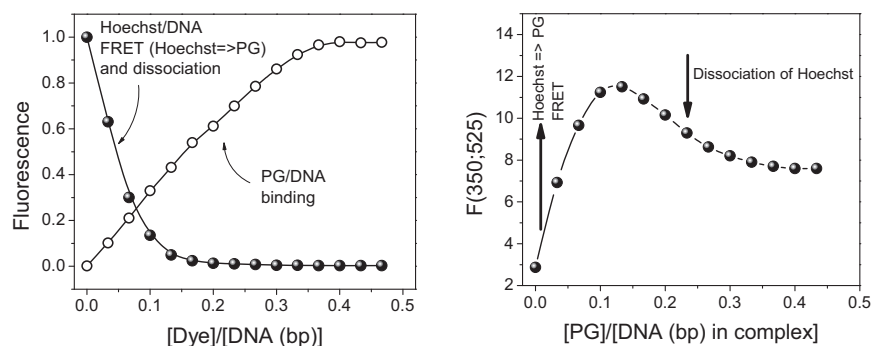


FIGURE 6 (Left) Dependence of fluorescence intensity of Hoechst 33258 (excitation at 350 nm; fluorescence measured at 460 nm) and PG (excitation at 472 nm; fluorescence measured at 525 nm) upon titration of a Hoechst/DNA complex (Dye/DNA = 0.1) with PG. (Right) Dependence of the fluorescence intensity of PG (excitation at 350 nm; fluorescence measured at 525 nm) upon titration of a Hoechst/DNA complex (Dye/DNA = 0.1) with PG. PG, PicoGreen fluorophore.

is observed (Fig. 6, left, red curve). It should be noted that Hoechst has a significantly lower quantum yield when free in solution ( $Q_{\text{free}} = 0.015$ ), in comparison to that when bound to DNA, ( $Q_{\text{bound}} = 0.42$  (17)). Therefore, both resonance energy transfer to PG in the bound state and release of dye from DNA cause a decrease in Hoechst emission intensity (Fig. 6 (left)).

Finally, competition between PG and Hoechst for association with DNA indicates that PG binds to the DNA minor groove.

### The origin of PG fluorescence enhancement upon interaction with DNA

Association of PG with DNA causes a drastic increase in its fluorescence (4,7,17) and excited state lifetime (7). In a recently published article (7), based on a proportional change of the PG quantum yield and lifetime, we made the assumption that the quenching of PG fluorescence in its free state, in comparison to the bound state in complex with DNA, is a dynamic quenching process. Subsequently we have studied the PG/DNA system to derive a detailed model for fluorescence enhancement. One approach to understanding this interaction is to analyze the role of solution viscosity and polarity on the emission and lifetime of the fluorescent probe.

Fig. 7 (left) shows fluorescence decay traces of PG in complex with DNA, free in buffer and in glycerol. The excited state lifetime ( $\tau_w$ ) of PG in buffer is very short,  $\tau_w = 4 \pm 3$  ps,

but in complex with DNA it increases almost 1000-fold, reaching a value of  $4.4 \pm 0.01$  ns. It is notable that, in viscous glycerol solution, the lifetime becomes dramatically longer than in water ( $\langle\tau_G\rangle = 0.75 \pm 0.02$  ns)—i.e., increases  $\sim 180$ -fold. Similarly, the quantum yield of the PG in glycerol is enhanced  $\sim 170$ -fold (Fig. 7 (right)). However, in ethanol, the lifetime of PG is even shorter than in water,  $<4$  ps—i.e., below the measurable lifetime range of the time-domain instrument. This result suggests that the change in solvent viscosity, but not its polarity and properties, is responsible for the dramatic fluorescence/lifetime changes observed in PG/DNA binding experiments.

The observed proportionality between fluorescence quantum yield and PG lifetime in glycerol/water solutions suggests the dynamic nature of the quenching effect. One of the possible mechanisms of dynamic quenching is bimolecular collisional quenching. In this case, quenching is diffusion-controlled and strongly depends on the viscosity of the solvent. However, also in this case, the quenching effect is typically small when compared with the results obtained here for PG quenching. For example, oxygen can be a natural quencher of a fluorophore in water. If we assume that the rate of oxygen bimolecular collisional quenching is  $k_q \approx 1 \times 10^{10} \text{ M}^{-1} \text{ s}^{-1}$  (31), the total quenching effect of oxygen on PG fluorescence will be significantly less,  $<10$ . Of course, we cannot exclude this quenching component from the observed PG quenching but its contribution is probably  $<1\%$  of the total observed quenching.

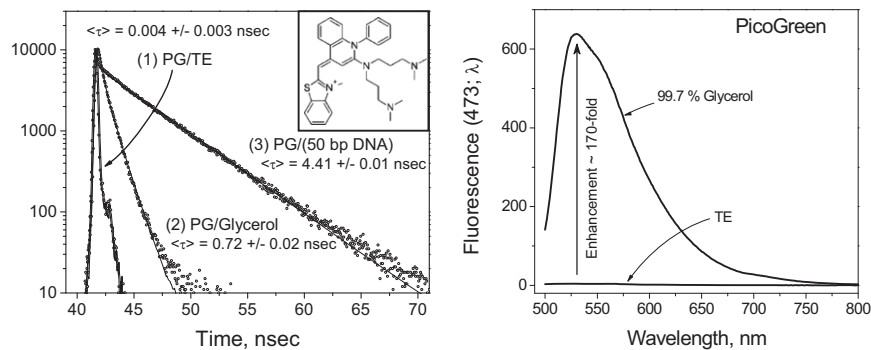


FIGURE 7 (Left) Fluorescence decay curves of free PG in TE buffer, in glycerol and in complex with DNA. Excitation of PG fluorescence was undertaken at 444 nm. The prompt (instrumental response function) is shown by the blue dots. (Right) Fluorescence spectra of PG in TE buffer and in glycerol.

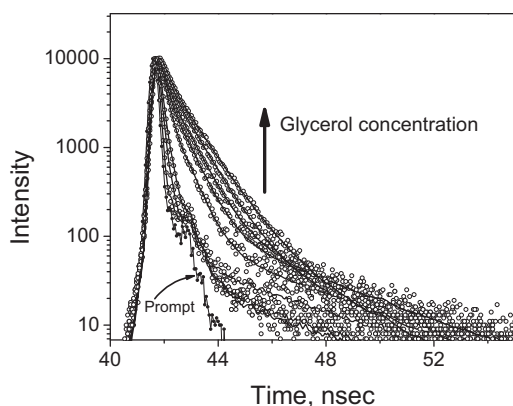


FIGURE 8 Fluorescence decay curves of PG in TE buffer and in solutions containing different concentrations of glycerol: 70, 80, 85, 90, 92, 96, 98, and 99.5% (w/w). Excitation was at 444 nm.

The most probable origin of PG fluorescence quenching/enhancement is intramolecular dynamics that result in perturbation of the thiazol-quinolinium coupled system. The unimolecular quenching constant,  $k_q$ , which characterizes intramolecular quenching effects, depends on the viscosity, which invariably reduces the rates of the internal dynamics of the PG molecule. Fig. 8 shows the decay of PG fluorescence intensity in solutions containing different concentrations of glycerol. The amplitude-weighted lifetimes,  $\langle\tau\rangle$ , calculated from these decay functions are plotted against viscosity (see Fig. 9 (left) and Table S1 in the Supporting Material). It should be noted that the lifetime of SG in glycerol/water solutions is very similar to that for PG, as expected from the high degree of structural similarity (Fig. 9 (left)). It is also notable that the curvature of the PG decay functions, which manifests dispersion in amplitudes and fluorophore lifetimes, are more pronounced in low viscosity (low concentration of glycerol) solutions and become more linear with viscosity increase.

It is well known that a high degree of dispersion in lifetime parameters is a characteristic of rapid intramolecular fluctuations that are comparable in timescale with the excited state lifetime of the chromophore. Under rigid

conditions, when the rate and amplitude of internal motions (deformations) are damped, the system exists as a distribution of a limited number of energetically favorable states (conformers). As a result, the fluorescence intensity decay function approaches a single exponential decay (see Fig. 8). Fig. 9 (right) shows the dependence of the lifetime upon viscosity, in  $1/\langle\tau\rangle$  versus  $T/\eta$  coordinates. Extrapolation of the function

$$1/\langle\tau\rangle = f(T/\eta) \text{ to } T/\eta = 0,$$

i.e., to infinite viscosity, gives the value of  $\langle\tau_0\rangle \approx 1$  ns. However, this value of the amplitude-weighted lifetime, which corresponds to a fully rigid state of the PG molecule, is  $\sim 4$  times shorter than that measured for PG in complex with DNA. It can be concluded that interaction of PG with DNA selects and stabilizes only one conformational state of the dye in the process of DNA complex formation. In the absence of distributions of PG isomers, the fluorescence decay function becomes linear—in fact, monoexponential (see Fig. S4).

## CONCLUSIONS

Based on the results of this study, we propose a model for PG/DNA complex formation. Fig. 10 (left) shows the structure of PG containing the three structural elements responsible for the different types of interaction with DNA: the phenyl-quinolinium and the benzo-thiazol aromatic systems, and the dimethylaminopropyl elongated chains. We assume that the quinolinium group of PG intercalates into DNA. This assumption is supported by theoretical considerations based on analysis of the induced circular dichroism signals from PG/DNA complexes (17). Tight contact of the quinolinium group between basepairs would be stabilized by van der Waals interactions with the DNA bases and rigidify this structural element on the DNA. As we have shown, the PG complex with DNA is stabilized by a charge-charge interaction. The PG benzo-thiazol group, that has one localized positive charge, is assumed responsible for the electrostatic

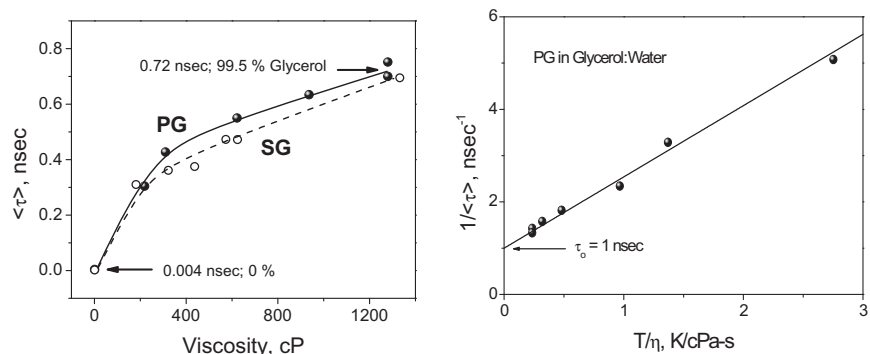


FIGURE 9 (Left) Dependence of amplitude-weighted excited state lifetime of free PG upon the solution viscosity. Data were calculated from the decay curves shown in Fig. 8. The decay parameters were extracted using least-squares impulse reconvolution analysis. (Right) The dependence of amplitude-weighted lifetimes upon viscosity in water-glycerol solutions. The value  $\tau_0 = 1$  ns is the lifetime of PG approximating to infinite viscosity ( $\eta$ ), i.e.,  $T/\eta = 0$ . PG, PicoGreen; SG, SYBR Green.

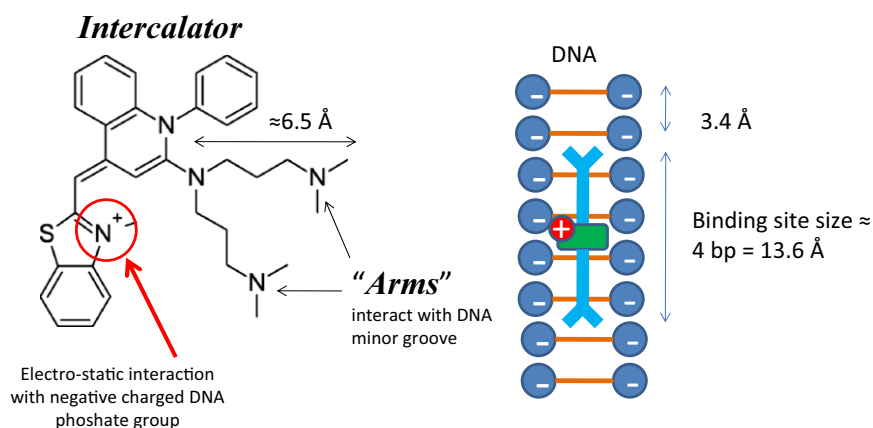


FIGURE 10 (Left) Structural elements of the PicoGreen molecule responsible for the different interactions with DNA. (Right) Model of the PG/DNA complex.

interaction with the DNA phosphate group. Being covalently bound to the quinolinium group and electrostatically to the DNA phosphate, it is to be expected that the thiazol also sits rigidly on the DNA, leading to a strong stabilization of the whole benzo-thiazol/quinolinium coupled system in a preferred conformational state. Consequently, in complex with the DNA duplex, PG exists in a defined conformational state and this conformer exhibits a single-exponential fluorescence decay function, i.e., high values of both the lifetime and quantum yield.

The results of our analysis have also shown that the binding site size of PG on a DNA duplex is nearly 4 bp, i.e.,  $\sim 13$  Å long. This site size is significantly longer than might be expected for just intercalation. Competition binding experiments with the minor groove binder, Hoechst 33258, show that PG also interacts with the minor groove of DNA. Therefore, taking into consideration the size of binding site and the fact of minor groove PG/DNA association, we suggest that the two dimethylaminopropyl groups, each of which in an extended conformation is  $\sim 6.5$  Å long, lie with their backbones deep in the minor groove, together covering a total of  $\sim 4$  bp of the duplex. These interactions contribute  $\sim 10$ – $12$  kJ/mol to the Gibbs energy of PG association with DNA, leading to an extremely strong binding constant.

## SUPPORTING MATERIAL

Table S1 and Figs. S1–S4 are available at [http://www.biophysj.org/biophysj/supplemental/S0006-3495\(10\)01113-6](http://www.biophysj.org/biophysj/supplemental/S0006-3495(10)01113-6).

The authors thank Professor Colyn Crane-Robinson, University of Portsmouth, Portsmouth, UK, for informative discussions.

The authors thank MedImmune for financial support. Support from the Institute of Fluorescence is also acknowledged.

## REFERENCES

- Ahn, S. J., J. Costa, and J. R. Emanuel. 1996. PicoGreen quantitation of DNA: effective evaluation of samples pre- or post-PCR. *Nucleic Acids Res.* 24:2623–2625.
- Schneeberger, C., P. Speiser, ..., R. Zeillinger. 1995. Quantitative detection of reverse transcriptase-PCR products by means of a novel and sensitive DNA stain. *PCR Methods Appl.* 4:234–238.
- Singer, V. L., L. J. Jones, ..., R. P. Haugland. 1997. Characterization of PicoGreen reagent and development of a fluorescence-based solution assay for double-stranded DNA quantitation. *Anal. Biochem.* 249:228–238.
- Zipper, H., H. Brunner, ..., F. Vitzthum. 2004. Investigations on DNA intercalation and surface binding by SYBR Green I, its structure determination and methodological implications. *Nucleic Acids Res.* 32:e103.
- Blaheta, R. A., B. Kronenberger, ..., B. H. Markus. 1998. Development of an ultrasensitive in vitro assay to monitor growth of primary cell cultures with reduced mitotic activity. *J. Immunol. Methods.* 211:159–169.
- Choi, S. J., and F. C. Szoka. 2000. Fluorometric determination of deoxyribonuclease I activity with PicoGreen. *Anal. Biochem.* 281:95–97.
- Dragan, A. I., E. S. Bishop, ..., C. D. Geddes. 2010. Metal-enhanced PicoGreen fluorescence: application for double-stranded DNA quantification. *Anal. Biochem.* 396:8–12.
- Murakami, P., and M. T. McCaman. 1999. Quantitation of adenovirus DNA and virus particles with the PicoGreen fluorescent dye. *Anal. Biochem.* 274:283–288.
- Noothi, S. K., M. Kombrabail, ..., G. Krishnamoorthy. 2009. Fluorescence characterization of the structural heterogeneity of polytene chromosomes. *J. Fluoresc.* 20:37–41.
- Noothi, S. K., M. Kombrabail, ..., B. J. Rao. 2009. Enhanced DNA dynamics due to cationic reagents, topological states of dsDNA and high mobility group box 1 as probed by PicoGreen. *FEBS J.* 276:541–551.
- Ikeda, Y., S. Iwakiri, and T. Yoshimori. 2009. Development and characterization of a novel host cell DNA assay using ultra-sensitive fluorescent nucleic acid stain “PicoGreen”. *J. Pharm. Biomed. Anal.* 49:997–1002.
- Geddes, C. D., and J. R. Lakowicz. 2002. Metal-enhanced fluorescence. *J. Fluoresc.* 12:121–129.
- Sobell, H. M., C. C. Tsai, ..., S. G. Gilbert. 1977. Visualization of drug-nucleic acid interactions at atomic resolution. III. Unifying structural concepts in understanding drug-DNA interactions and their broader implications in understanding protein-DNA interactions. *J. Mol. Biol.* 114:333–365.
- Reference deleted in proof.
- Dragan, A. I., R. Carrillo, ..., P. L. Privalov. 2008. Assembling the human IFN- $\beta$  enhanceosome in solution. *J. Mol. Biol.* 384:335–348.
- Lakowicz, J. R. 2006. Principles of Fluorescence Spectroscopy. Springer Science + Business Media, New York.

17. Cosa, G., K. S. Focsaneanu, ..., J. C. Scaiano. 2001. Photophysical properties of fluorescent DNA-dyes bound to single- and double-stranded DNA in aqueous buffered solution. *Photochem. Photobiol.* 73:585–599.
18. McGhee, J. D., and P. H. von Hippel. 1974. Theoretical aspects of DNA-protein interactions: co-operative and non-co-operative binding of large ligands to a one-dimensional homogeneous lattice. *J. Mol. Biol.* 86:469–489.
19. Dragan, A. I., J. R. Liggins, ..., P. L. Privalov. 2003. The energetics of specific binding of AT-hooks from HMGA1 to target DNA. *J. Mol. Biol.* 327:393–411.
20. Manning, G. S. 1978. The molecular theory of polyelectrolyte solutions with applications to the electrostatic properties of polynucleotides. *Q. Rev. Biophys.* 11:179–246.
21. Record, Jr., M. T., C. F. Anderson, and T. M. Lohman. 1978. Thermodynamic analysis of ion effects on the binding and conformational equilibria of proteins and nucleic acids: the roles of ion association or release, screening, and ion effects on water activity. *Q. Rev. Biophys.* 11:103–178.
22. Record, Jr., M. T., W. Zhang, and C. F. Anderson. 1998. Analysis of effects of salts and uncharged solutes on protein and nucleic acid equilibria and processes: a practical guide to recognizing and interpreting polyelectrolyte effects, Hofmeister effects, and osmotic effects of salts. *Adv. Protein Chem.* 51:281–353.
23. Crane-Robinson, C., A. I. Dragan, and P. L. Privalov. 2006. The extended arms of DNA-binding domains: a tale of tails. *Trends Biochem. Sci.* 31:547–552.
24. Dragan, A. I., C. M. Read, ..., P. L. Privalov. 2004. DNA binding and bending by HMG boxes: energetic determinants of specificity. *J. Mol. Biol.* 343:371–393.
25. Privalov, P. L., A. I. Dragan, ..., C. A. Minetti. 2007. What drives proteins into the major or minor grooves of DNA? *J. Mol. Biol.* 365:1–9.
26. Lippard, S. J. 1978. Platinum complexes—probes of polynucleotide structure and anti-tumor drugs. *Acc. Chem. Res.* 11:211–217.
27. Kovacic, R. T., and K. E. van Holde. 1977. Sedimentation of homogeneous double-strand DNA molecules. *Biochemistry.* 16:1490–1498.
28. Haq, I., J. E. Ladbury, ..., J. B. Chaires. 1997. Specific binding of Hoechst 33258 to the d(CGCAAATTTGCG)<sup>2</sup> duplex: calorimetric and spectroscopic studies. *J. Mol. Biol.* 271:244–257.
29. Utsuno, K., Y. Maeda, and M. Tsuboi. 1999. How and how much can Hoechst 33258 cause unwinding in a DNA duplex? *Chem. Pharm. Bull. (Tokyo).* 47:1363–1368.
30. Pjura, P. E., K. Grzeskowiak, and R. E. Dickerson. 1987. Binding of Hoechst 33258 to the minor groove of B-DNA. *J. Mol. Biol.* 197:257–271.
31. Lakowicz, J. R., and G. Weber. 1973. Quenching of fluorescence by oxygen. A probe for structural fluctuations in macromolecules. *Biochemistry.* 12:4161–4170.